

PAPER • OPEN ACCESS

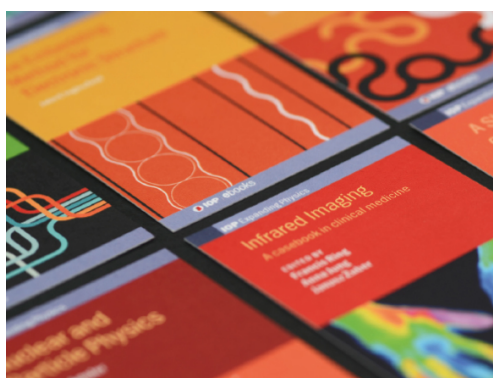
Rubidium atom spectral lineshapes in high intensity light fields near an optical nanofibre

To cite this article: Vandna Gokhroo *et al* 2022 *J. Phys. B: At. Mol. Opt. Phys.* **55** 125301

View the [article online](#) for updates and enhancements.

You may also like

- [Japanese population dose from natural radiation](#)
Yasutaka Omori, Masahiro Hosoda, Fumiaki Takahashi *et al.*
- [Measurement techniques for multiphase flows](#)
Koji Okamoto and Yuichi Murai
- [Temperature measurement of cold atoms using transient absorption of a resonant probe through an optical nanofibre](#)
Ravi Kumar, Vandna Gokhroo, Vibhuti Bhushan Tiwari *et al.*



IOP | ebooks™

Bringing together innovative digital publishing with leading authors from the global scientific community.

Start exploring the collection—download the first chapter of every title for free.

Rubidium atom spectral lineshapes in high intensity light fields near an optical nanofibre

Vandna Gokhroo^{1,*} , Fam Le Kien¹  and Síle Nic Chormaic^{1,2,*} 

¹ Okinawa Institute of Science and Technology Graduate University, Onna, Okinawa 904-0495, Japan

² Laboratoire de Physique des Gaz et des Plasmas, CNRS, Université Paris-Saclay, 91405 Orsay, France

E-mail: vandna.gokhroo@mahindrauniversity.edu.in and sile.nicchormaic@oist.jp

Received 31 January 2022, revised 14 April 2022

Accepted for publication 28 April 2022

Published 24 May 2022



Abstract

The integration of cold atomic systems with optical nanofibres (ONFs) is an increasingly important experimental platform. Here, we report on the spectra observed during a strongly driven, single-frequency, two-photon excitation of cold rubidium atoms near an ONF. At resonance, two competitive processes, namely a higher excitation rate and stronger pushing of atoms from the nanofibre due to resonance scattering, need to be considered. We discuss the processes that lead to the observed two-peak profile in the fluorescence spectrum as the excitation laser is scanned across the resonance, noting that the presence of the ONF dramatically changes the fluorescence signal. These observations are useful for experiments where high electric field intensities near an ONF are needed, for example when driving nonlinear processes.

Keywords: lineshapes, intensity, optical nanofibre, two-photon excitation, cold atoms

(Some figures may appear in colour only in the online journal)


1. Introduction

Interactions between atoms and laser fields have been widely studied in many different scenarios, such as a two-level atom interacting with a monochromatic laser field, a three-level atom interacting with two laser fields, multilevel atoms with multi-frequency light fields [1, 2], etc. The presence of coherence in such systems can substantially enhance the optical nonlinearity, leading to many interesting effects such as electromagnetically induced transparency and coherent population trapping [3–5]. Over the past decade, optical waveguides, including optical nanofibres (ONFs), have come to the fore as an ideal platform to study interactions of atoms with light. We focus our discussion on ONFs, which provide tight

confinement of light beyond the Rayleigh range and also serve as an ideal channel for light propagation. ONFs have been used to efficiently probe, manipulate and trap cold, alkali atoms [6–10] with recent works extending atom and ONF studies to the observation of a quadrupole transition in ⁸⁷Rb atoms [11], the demonstration of quadrature squeezing of nanofibre-guided light [12], and a determination of the polarization dependency of spin selection in laser-cooled atoms [13].

Many experiments involving two-photon processes demand minimizing the one-photon excitation. A larger detuning of the excitation laser frequency with respect to the intermediate level leads to fewer atoms in it at the expense of a higher light field intensity requirement. In single-frequency, two-photon excitation, in general, the laser frequency is very far-detuned from the intermediate levels; additional advantages are the need for only one laser and a more straightforward theoretical description. The subwavelength diameter of an ONF provides very high intensities in the evanescent field at very low powers (e.g. a few nW of propagating light can produce a Rabi frequency of

* Authors to whom any correspondence should be addressed.

 Original content from this work may be used under the terms of the [Creative Commons Attribution 4.0 licence](https://creativecommons.org/licenses/by/4.0/). Any further distribution of this work must maintain attribution to the author(s) and the title of the work, journal citation and DOI.

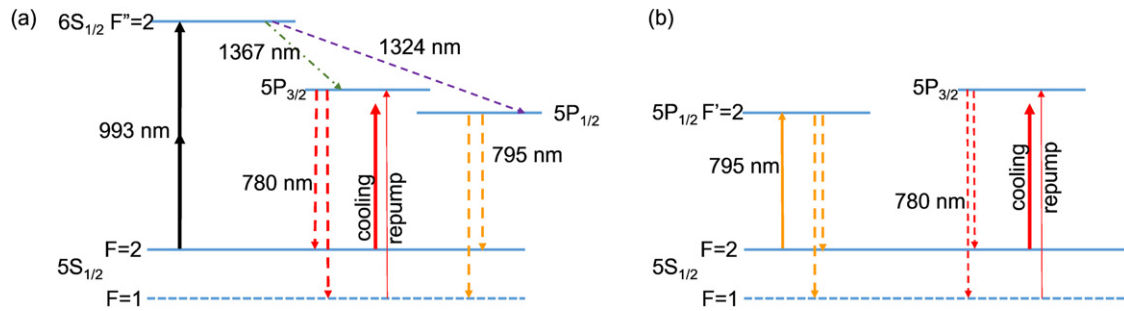


Figure 1. Energy level diagrams for ^{87}Rb . Cold atoms are prepared in a MOT using cooling and repump beams around 780 nm. Excitation (solid arrows) and decay (dashed arrows) channels are shown. (a) 993 nm light excites atoms from the $5S_{1/2} F = 2$ state to the $6S_{1/2} F'' = 2$ state using a two-photon process. Atoms decay to $5S_{1/2} F = 1, 2$ via the $5P_{3/2}$ and $5P_{1/2}$ intermediate levels by emitting 780 nm or 795 nm photons in the lower decay stage. (b) 795 nm light excites atoms from the $5S_{1/2} F = 2$ state to the $5P_{1/2} F' = 2$ state using a one-photon process. Atoms decay to $5S_{1/2} F = 1, 2$ by emitting 795 nm photons.

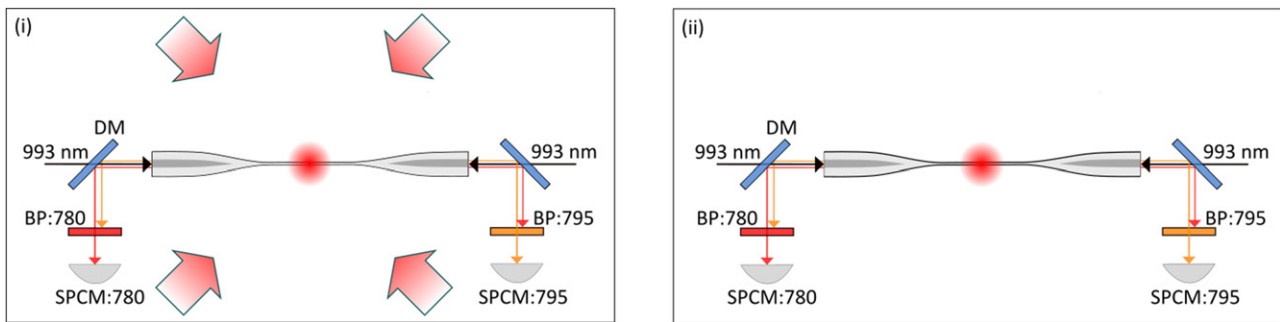


Figure 2. Experimental setup for configuration I. Two-photon excitation at 993 nm (i) with and (ii) without the MOT cooling beams. SPCM: single-photon counting module; BP: bandpass filter; DM: dichroic mirror. The repump beam is kept on at all times.

tens of MHz for atoms in the evanescent field [14]), hence providing near-ideal conditions for single-frequency, two-photon excitation to occur. However, there is also a disadvantage since the origin of some observed effects on spectral lineshapes due to the presence of the ONF is not always clear [15–18].

In this work, we generate high electric field intensities using either an ONF or a tightly focussed free-space beam, so as to make a comparison between the observed effects on spectral line shapes. Notably, the fluorescence signal from atoms near an ONF can exhibit a two-peak profile as the frequency of the excitation laser is scanned across an atomic resonance. We explore several atomic transitions and experimental configurations to investigate this effect in detail and hypothesise on possible sources of the observed phenomenon.

2. Experimental details

We prepared an ensemble of trapped cold ^{87}Rb atoms using a standard magneto-optical trap (MOT) setup [13]. The average temperature of the atomic cloud was $\sim 200 \mu\text{K}$, with a density of $10^{10} \text{ atoms cm}^{-3}$. The cooling beams for the MOT were 14 MHz red-detuned from the $5S_{1/2} F = 2 \rightarrow 5P_{3/2} F' = 3$ transition with an intensity of $\sim 11 \text{ mW cm}^{-2}$ per beam. The ONF was fabricated from commercial step-index optical fibre (Fibercore, SM800-5.6-125) by heating it with an oxygen–hydrogen flame and simultaneously pulling it using computer-controlled motorised stages [19]. The final nanofibre waist was $\sim 400 \text{ nm}$, allowing only fundamental mode

propagation for all the wavelengths used in the experiment, 780 nm, 795 nm, and 993 nm. Note that all ONF-guided excitation laser powers mentioned were measured at the output pigtail of the ONF and the power at the waist could be somewhat higher due to propagation losses in the fiber.

Experiments were performed in two configurations with atoms being excited via a two-photon transition or a one-photon transition, see figure 1. Resonant and near-resonant excitation of the atoms was achieved using a sub-MHz linewidth Ti-sapphire laser (M Squared Lasers: SolsTis ECD-X). Fluorescence photons during the de-excitation process coupled into the ONF and propagated to the pigtail on either end where they were subsequently detected using single-photon counter modules (SPCM: Excelitas Technologies: SPCM-AQRH-14-FC), see figure 2. Dichroic mirrors and interference filters were used to combine and separate the different wavelengths as per experimental requirements. Additionally, the fluorescence signal from the cold atom cloud could be collected in free-space via a microscope composed of two convex lenses, with focal lengths of 125 mm and 250 mm, and was measured using a photomultiplier tube (PMT: Hamamatsu Photonics), see figure 3. Both the lenses and the PMT were kept outside the vacuum chamber.

2.1. Configuration I: single-frequency, two-photon excitation around the optical nanofibre

We used 993 nm light to excite ^{87}Rb atoms from $5S_{1/2} F = 2 \rightarrow 6S_{1/2} F'' = 2$ using a two-photon process, see figure 1(a). The

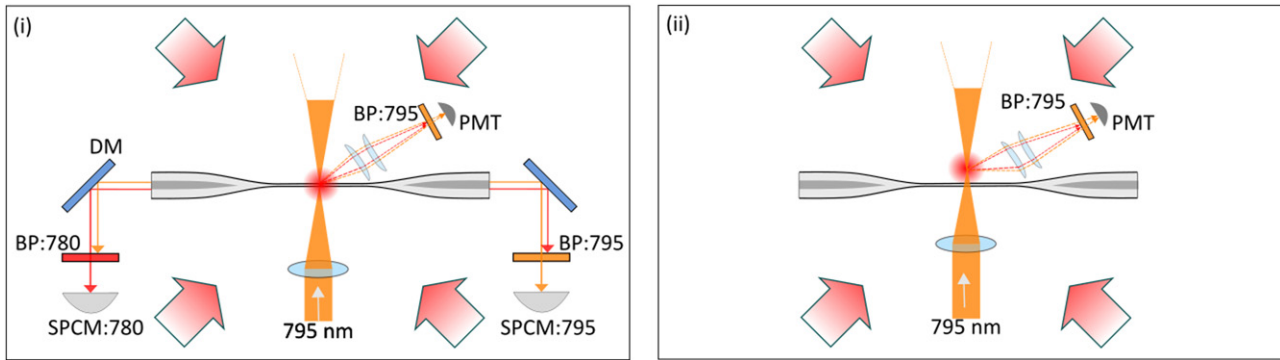


Figure 3. Experimental setup for configuration II. One-photon excitation at 795 nm with the cold atom cloud (i) around the ONF and (ii) removed from the ONF. SPCM: single-photon counting module; PMT: photomultiplier tube; BP: bandpass filter; DM: dichroic mirror.

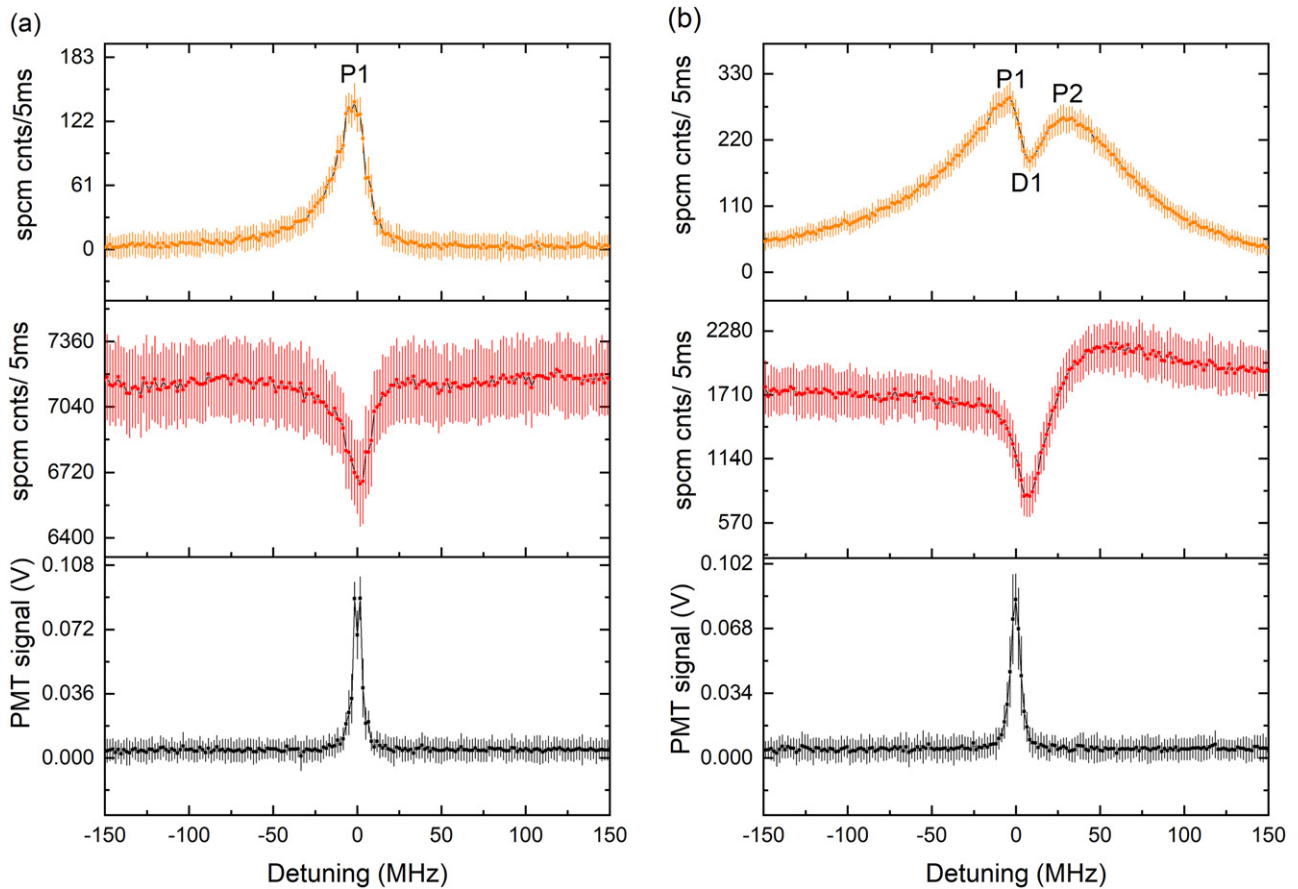


Figure 4. Excitation light at 993 nm, going through the ONF in both directions, is scanned across the $5S_{1/2} F = 2 \rightarrow 6S_{1/2} F'' = 2$ transition via two-photon excitation. Total power of 993 nm excitation light in the ONF is (a) 0.1 mW and (b) 2.45 mW. From top to bottom: 795 nm fluorescence signal coupled into the ONF, 780 nm fluorescence signal coupled into the ONF, spectroscopy signal from a Rb vapour cell recorded on a PMT for the frequency reference. Typical laser power used for the vapour cell spectroscopy was ~ 100 mW.

993 nm light was obtained from the Ti-sapphire laser and could be frequency scanned or locked. Excited atoms in the $6S_{1/2}$ state spontaneously decayed to the ground state, $5S_{1/2} F = 1, 2$, via (i) the intermediate state, $5P_{1/2}$, by emitting a 1324 nm photon followed by a 795 nm photon or (ii) the intermediate state, $5P_{3/2}$, by emitting a 1367 nm photon followed by a 780 nm photon. The ratio of the transition rates of $6S_{1/2} \rightarrow 5P_{1/2}$ to $6S_{1/2} \rightarrow 5P_{3/2}$ is 0.48 and $5P_{3/2} \rightarrow 5S_{1/2}$ to $5P_{1/2} \rightarrow 5S_{1/2}$ is 1.04 [20]. Hence, it is almost twice as likely that 780 nm

photons are emitted in the decay process from $6S_{1/2}$ to $5S_{1/2} F = 1, 2$ than 795 nm photons.

2.2. Configuration II: one-photon excitation in a cold atom cloud

To better understand the two-photon excitation experiments, we also performed one-photon excitation experiments. Cold atoms in the MOT were excited from the $5S_{1/2} F = 2$ state to the $5P_{1/2} F' = 2$ state via 795 nm light (~ 377.10519 THz), see

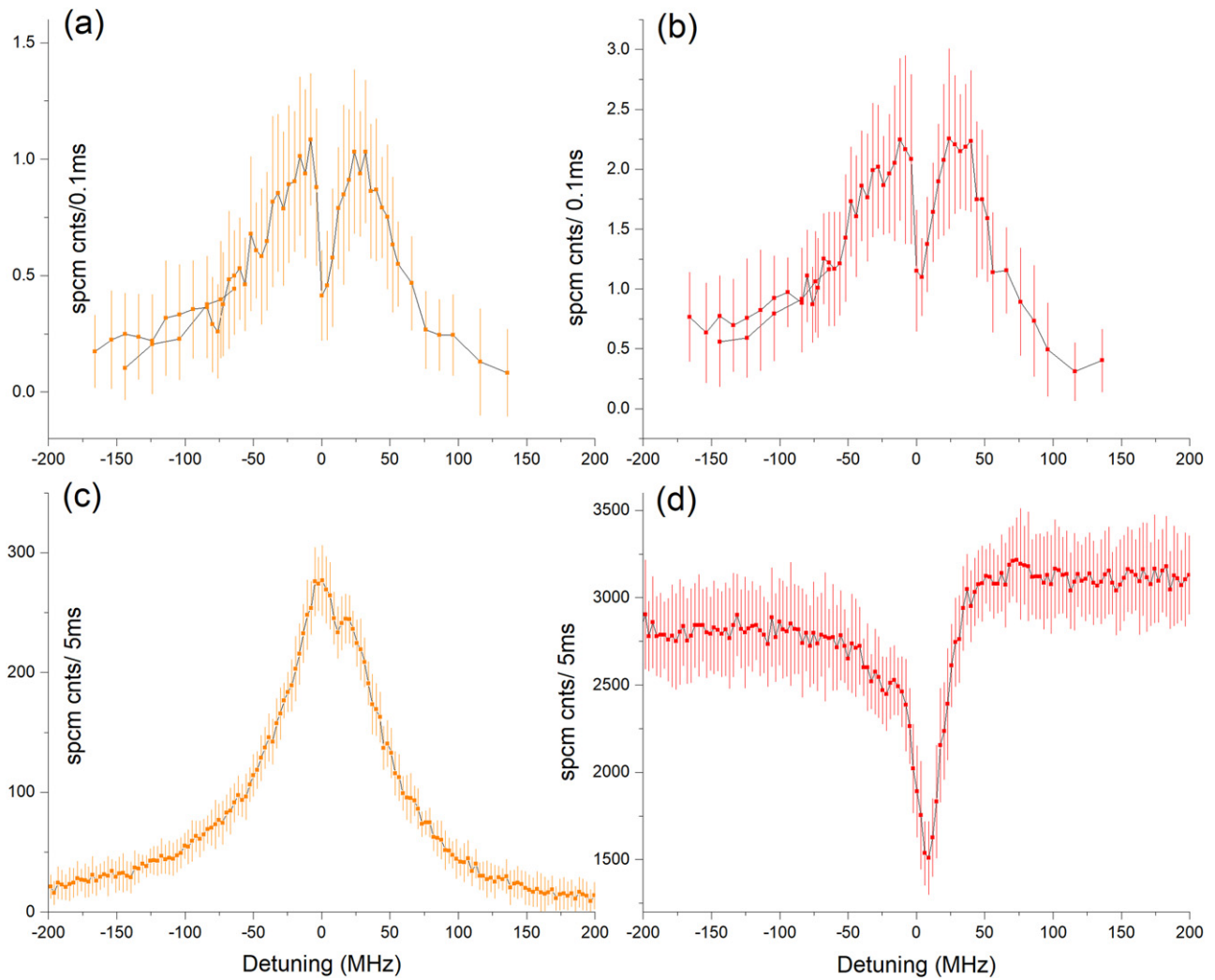


Figure 5. Fluorescence signal during two-photon excitation at 993 nm. Comparison of 795 nm (left plots in orange) and 780 nm (right plots in red) fluorescence signals in the absence (a) and (b) and in the presence (c) and (d) of cooling light. Excitation light through the ONF was kept at 2 mW.

figure 1(b). Since the excitation and the fluorescence light were of the same wavelength, sending the excitation light through the ONF and detecting the fluorescence signal using a SPCM, was not suitable. Instead, we used a free-space beam at 795 nm, focussed on the cold atom cloud via a convex lens (Thorlabs: LB1779-B, $f = 30$ cm). The excitation light at 795 nm was derived from the Ti-sapphire laser and could be scanned or locked at a fixed frequency.

3. Experimental results

3.1. Configuration I: single-frequency, two-photon excitation around the optical nanofibre

3.1.1. Cooling beams on. In the first test, 993 nm excitation light was sent through the ONF and fluorescence measurements were made in the presence of the MOT i.e. with cooling and repump beams on. The 993 nm light was frequency-scanned across the $5S_{1/2} F = 2 \rightarrow 6S_{1/2} F'' = 2$ resonance (~ 301.77791 THz). The fluorescence signals at 795 nm and 780 nm coupled into the ONF and were measured at the

SPCMs, see figure 2(i). In this scenario, fluorescence at 780 nm had contributions from both the excitation process to the $6S_{1/2} F'' = 2$ state (via one of the decay channels) and the MOT beams exciting atoms to the $5P_{3/2} F'$ states. In contrast, detected fluorescence photons at 795 nm were solely due to the $6S_{1/2} F'' = 2$ state excitation, see the level diagram in figure 1(a).

For a low power (0.1 mW) of the 993 nm excitation light propagating through the ONF, as the laser is tuned on-resonance with the $5S_{1/2} F = 2 \rightarrow 6S_{1/2} F'' = 2$ two-photon resonance condition, we observe a peak (P1) in the 795 nm fluorescence and a corresponding dip in the 780 nm fluorescence signal coupled into the nanofibre, see top and middle panels of figure 4(a). Detuning is defined as twice the laser frequency minus the atomic transition frequency for $5S_{1/2} F = 2 \rightarrow 6S_{1/2} F'' = 2$. With an increase in the 993 nm power to 2.45 mW, the 795 nm fluorescence signal shows a dip, D1, and the appearance of a second peak, P2, as shown in the top panel of figure 4(b). P2 becomes more pronounced with an increase

in the 993 nm power; the two peaks, P1 and P2, also move further apart, i.e., the dip appears to become broader. The dip in the 780 nm signal is at exactly the same frequency as the dip in the 795 nm signal, see the top and middle panels of figure 4(b). The dip appears at a slightly positive detuning (by 1 to 7 MHz). Frequency calibration was obtained via simultaneous measurement using a wavemeter (HighFinesse GmbH WS8-2) in conjunction with spectroscopy performed in a Rb vapour cell with natural isotope abundance. The vapour cell was heated to ~ 100 °C. Counterpropagating 993 nm laser beams passing through the cell cancelled the first-order Doppler shift and provided us with a Doppler-free spectroscopy peak as a precise frequency reference [21]. The full-width-at-half-maximum of the vapour cell signal is ~ 6 MHz, see bottom panels of figure 4. The fluorescence signal obtained from the cold atoms near the ONF was typically much broader (~ 20 MHz) than the vapour cell signal, which we attribute to surface effects from the ONF [18, 22]. We also observed that the splitting was more pronounced when the cloud was less dense (data not shown).

3.1.2. Cooling beams off. To simplify the system, we next ran a series of tests with the cooling beams at 780 nm switched off during data acquisition and 2 mW of 993 nm excitation power going through the ONF, see figure 2(ii). Here, the fluorescence signals at 795 nm and 780 nm were mainly from the $6S_{1/2} F'' = 2$ decay channels. Though some repump signal could contribute we assumed this was negligible. The experimental sequence was as follows: 993 nm light was sent through the ONF and its frequency was locked near or on resonance. The cold atom cloud was initially prepared in the MOT and this was followed by a polarisation gradient cooling phase (bringing the cooling power per beam from 11 mW cm^{-2} to 2.7 mW cm^{-2} and the cooling beam detuning from -14 MHz to -30 MHz) for 5 ms. Subsequently, the cooling beams were turned off before the measurements. The fluorescence signal was collected during the first $700 \mu\text{sec}$ and averaged over 20 cycles. A full spectrum was obtained by scanning the locking point of the 993 nm laser in steps of ~ 2 MHz across the resonance and repeating the procedure as described above for each frequency step.

For the experiments presented in figure 4, the cooling beams were on at all times. By running the experiments in the absence of cooling beams, we could eliminate the possibility of Autler–Townes splitting being the cause for the observed split profiles. In the absence of the cooling beams, the observed fluorescence signals at 780 nm and 795 nm show similar trends with different amplitudes, see figures 5(a) and (b). This is expected since both signals are from the de-excitation of the $6S_{1/2} F'' = 2$ state to the $5S_{1/2} F = 1, 2$ states albeit with different transition probabilities. For comparison, fluorescence signals at 780 nm and 795 nm in a MOT, i.e., with the cooling beams on, are also plotted, see figures 5(c) and (d). Comparing figures 5(a) and (c), we see that the splitting is present in both the cases though it is more pronounced and the dip is deeper in the absence of cooling beams compared with the signals obtained with cooling beams.

Finally, in figure 6, the fluorescence signal at 795 nm for different 993 nm powers, in the absence of cooling beams, is

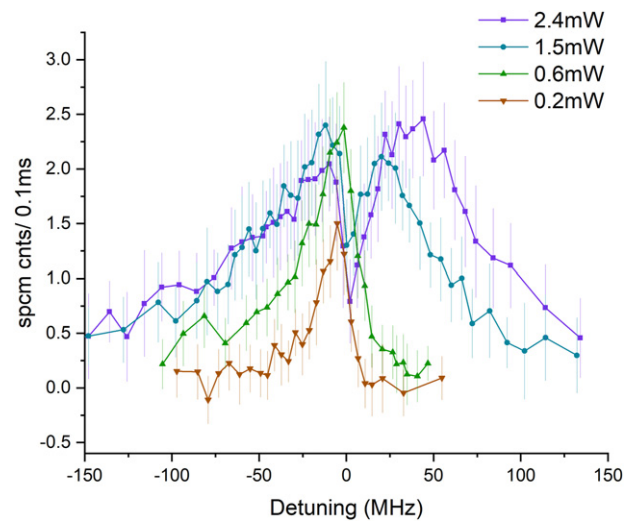


Figure 6. Fluorescence at 795 nm from the cold atoms near the ONF during two-photon excitation in the absence of the cooling beams. Signals are compared for different excitation powers.

plotted. Similar to the results presented in the top panels of figures 4(a) and (b), we observe a two-peak profile and the dip becomes more pronounced as the 993 nm power is increased.

3.2. Configuration II: one-photon excitation in a cold atom cloud

3.2.1. Cold atoms around the ONF. The intriguing two-peak profiles observed in the two-photon excitation experiments were investigated by comparing the results with two different, one-photon excitation measurements. The first was when the MOT was formed around the ONF while the free-space focussed excitation beam at 795 nm, transverse to the ONF, was sent through the atomic cloud, see figure 3(i). As the frequency of the 795 nm was scanned across the resonance $5S_{1/2} F = 2 \rightarrow 5P_{1/2} F' = 2$, the fluorescence signals at 795 nm and 780 nm were measured using SPCMs and a PMT. Note that fluorescence photons, which coupled into the ONF, were detected via the SPCM, see figure 3(i). The observed spectra are shown in figures 7(a) and (b) where detuning is defined as the laser frequency minus the atomic transition frequency for $5S_{1/2} F = 2 \rightarrow 5P_{1/2} F' = 2$. The fluorescence at 795 nm, see figure 7(a), exhibits two dominant peaks (P1 and P2) and a dip (D1) as the 795 nm excitation laser was detuned from resonance. The spectra also show a small dip (D2) and a peak (P3). Peak P2 becomes more prominent as the 795 nm excitation power is increased and P1, P2 and D1 become broader, see figure 7(a). Fluorescence was also measured at the PMT without being coupled to the ONF, see figure 3(i) for the experimental setup. When we compare the fluorescence signals measured at the PMT and the SPCM, see figure 8(a), we observe that the PMT signal is narrower and shows a dip at the same position as the SPCM signal. These observations show that, similar to the two-photon excitation scenario, here also the two peaks, P1 and P2, move apart or the dip, D1, becomes broader as the excitation power is increased.

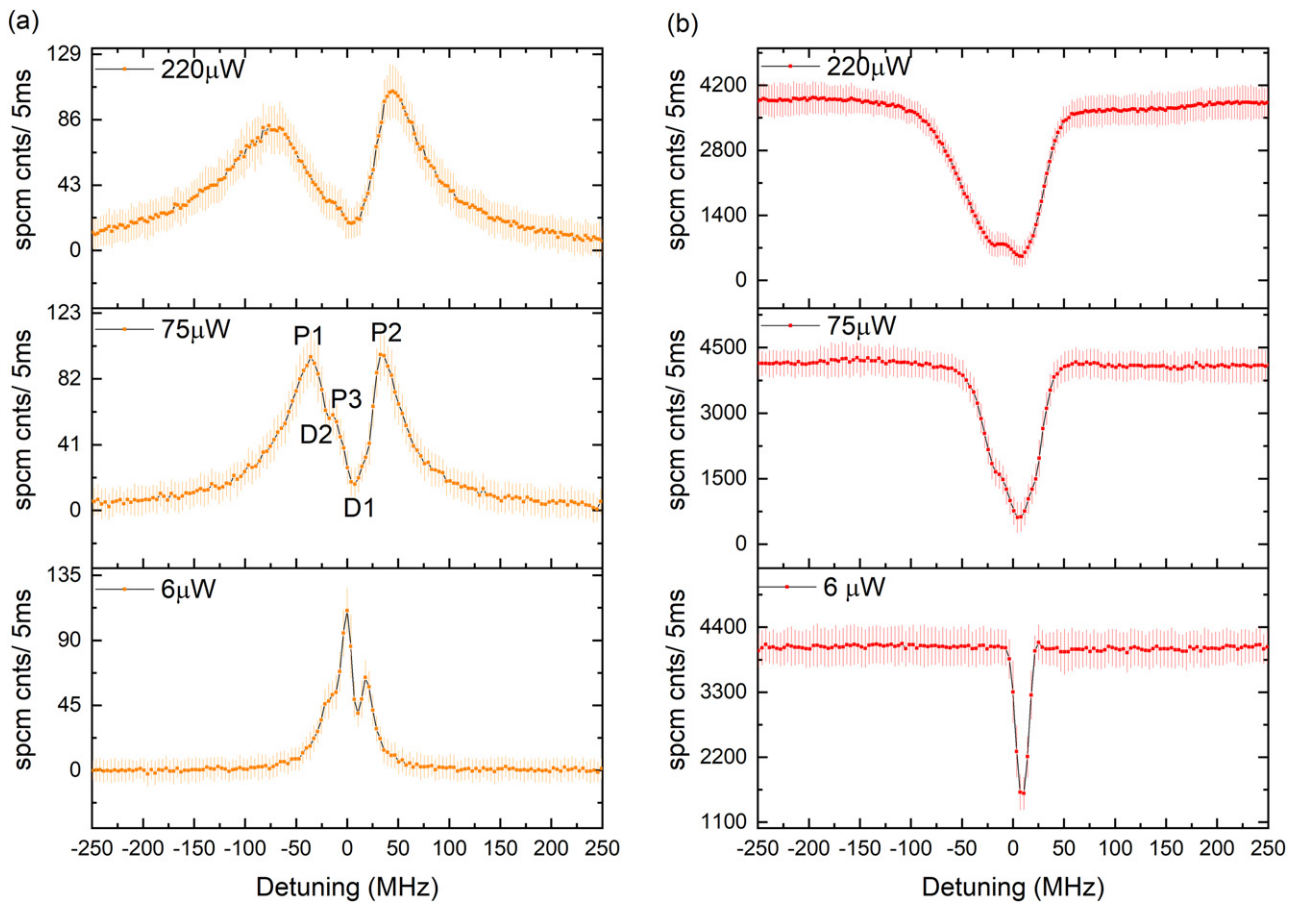


Figure 7. Fluorescence signals from the MOT during one-photon excitation at 795 nm. (a) 795 nm fluorescence signal for different excitation powers of 795 nm. (b) 780 nm fluorescence signal for different excitation powers of 795 nm.

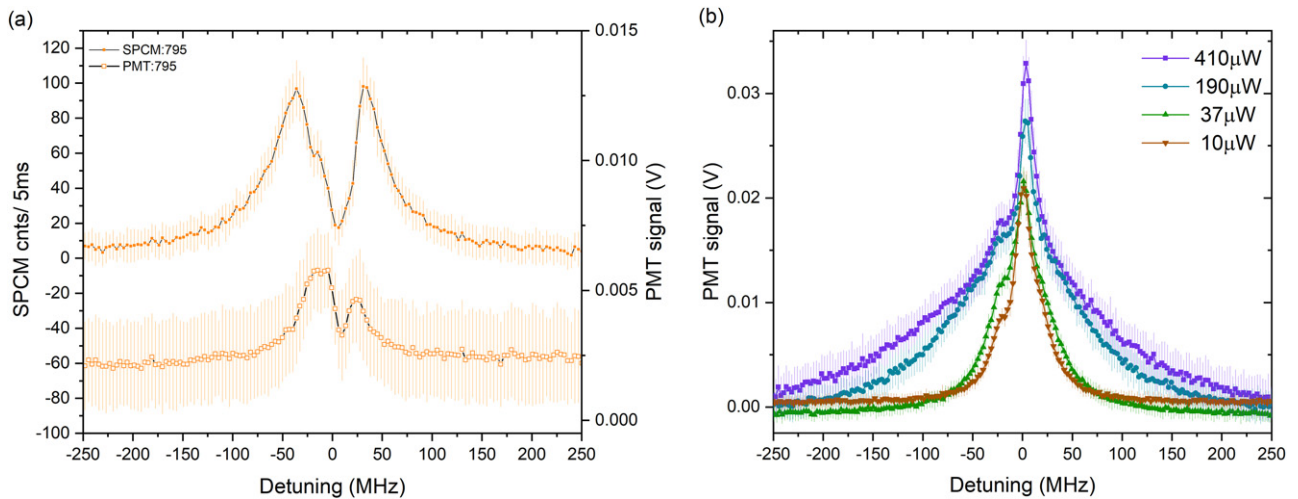


Figure 8. (a) One-photon excitation signal when the cold atom cloud overlaps the ONF. Comparison of 795 nm signals collected from the PMT and the SPCM are shown by empty (bottom curve) and solid (top curve) circle data points, respectively. (b) One-photon excitation when the cold atom cloud is far from the ONF. Fluorescence signal at 795 nm on the PMT is plotted for different excitation powers.

3.2.2. Cold atoms distant from the ONF. The second one-photon experiment we considered was when the cold atom cloud was distant from the ONF, see figure 3(ii), to ensure that there was no coupling of the fluorescence signal into the nanofibre. This was achieved by changing the current in one of the MOT anti-Helmholtz coils, thereby shifting the zero of the

magnetic field, hence the trap position. The excitation beam was realigned so that it passed through the atom cloud. The fluorescence signal at 795 nm as a function of the excitation laser detuning from $5S_{1/2} F = 2 \rightarrow 5P_{1/2} F' = 2$ transition, see figure 1(b), was collected by the PMT. In figure 8(b), the fluorescence signal at 795 nm while varying the 795 nm excitation

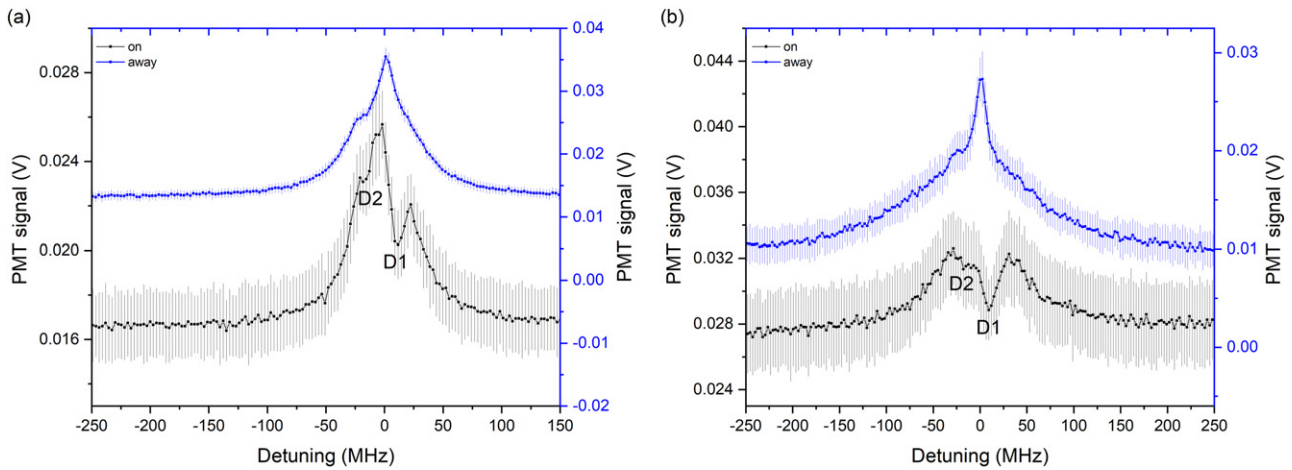


Figure 9. Comparison of 795 nm fluorescence signal at the PMT during one-photon excitation. Data in blue show the signal when MOT is formed away from the ONF and data in black show when MOT is on the ONF. Excitation powers are $\sim 37 \mu\text{W}$ and $\sim 150 \mu\text{W}$ for (a) and (b), respectively.

laser frequency is plotted for different excitation powers. Even at higher powers ($410 \mu\text{W}$) a second peak does not appear in the spectra. Additionally, the observed fluorescence profile is not Lorentzian.

Finally, to compare the observed spectra when the atom cloud overlaps the ONF and when the cloud is removed from the ONF, we measured the 795 nm fluorescence signals for the same excitation powers. The results are plotted in figure 9 for two different excitation powers and show the striking contrast between the two cases. Notably, the two-peak profile is present only when both the cold atom cloud and the focussed, strong excitation beam are at the ONF. In both these cases, the 795 nm excitation light was focussed at the atom cloud via the lens.

4. Discussion

Results show that, for both one- and two-photon excitation processes near an ONF, high intensities of the evanescent field produce a two-peak profile in the fluorescence signal as a function of laser detuning. The similarity of the profiles in the two cases suggests that the origin is not linked with any process specific to the one- or two-photon excitation phenomena. To better understand the observed structure, we considered the feasibility of the shape arising from certain phenomena to hypothesise on the exact origin.

As a first line of investigation, we considered whether the lineshape could arise from interference. Subnatural linewidth spectral lines have already been investigated theoretically and experimentally both in V-type and Λ -type atomic systems in the presence of two laser fields [23, 24]. Quantum interference between the two transition pathways plays a crucial role in producing such narrow spectral features. Interference can also be present when monochromatic light couples a single atomic ground state to two closely spaced excited states by parallel dipole moments. At an appropriate frequency of the excitation laser field, fluorescence from the excited levels can be eliminated [25]. However, the condition of parallel dipole moments cannot be fulfilled when considering two closely spaced

Zeeman sublevels of a particular hyperfine state, hence making it nontrivial to achieve. It has also been proposed that anisotropy of the vacuum field could provide the necessary condition for quantum interference among closely lying states [26]. Since the two observed peaks are far-separated even at zero magnetic field, we rule out this possibility. In summary, interference cannot give a satisfactory answer for the origin of the two-peak profile. Cooperative effects, such as the Dicke effect, do not seem to be present in the system because the two-hump feature was robust. It was present on varying the MOT cooling beam intensities, detunings, and excitation laser powers. In addition, the fluorescence did not seem to be directional, so we did not perform any time-resolved measurements. We also eliminated the possibility of mode interference within the nanofibre because, as stated earlier, only the fundamental mode (Gaussian field profile) could propagate for all the wavelengths used in the experiment, i.e., 780 nm, 795 nm, and 993 nm.

Another possibility we considered was that of Autler–Townes splitting [14] caused by the strong laser cooling beams; however, we have also ruled this out because the splitting is present even in the absence of the cooling beams and theoretical models do not support this possibility.

We propose that the actual phenomenon is far simpler than initially assumed. The observed spectra can be explained by considering the pushing effect of the excitation light, i.e., 993 nm or 795 nm laser light, on the atoms. As the light frequency approaches the atomic resonance, the photon absorption rate increases. Atoms in the highest intensity region are pushed away maximally due to momentum kicks given by the photons. This leads to a reduced atom density locally and, thereby, reduced fluorescence. In addition, we also need to consider that the atomic resonance or the resonant transition frequency in a MOT is modified due to the ac Stark effect of the cooling beams. These new resonance frequencies will be referred henceforth as the modified resonances. The experiments in the absence of cooling beams also initially relied on having a MOT, i.e., cooling light, in the presence of a

frequency-locked excitation beam passing through the ONF (see subsection 3.1.2). Due to the aforementioned pushing effect, the initial atom number near the ONF depends on the excitation frequency and is not the same for each frequency step during the scan. This leads to low fluorescence whenever the frequency of the excitation light matches to the modified resonances, even though fluorescence was collected in the absence of the cooling beams. In the following, to understand the frequency values or positions of the modified resonances, we consider the ac Stark effect of the cooling beams on both the ground ($5S_{1/2} F = 2$) and the excited ($5P_{3/2} F' = 3$) states of an ^{87}Rb atom. The new energy eigenstates can be calculated using the dressed atom picture [1].

To compare with the bare atom energy states, we consider the specific case of a red-detuned light field, such as the MOT cooling beams in our experiments. In this case, both the ground and the excited states split into two dressed states. The two dressed ground states are shifted in frequency by $\Delta_{1g} = -(\Omega_c - |\delta_c|)/2$ and $\Delta_{2g} = (\Omega_c + |\delta_c|)/2$ w.r.t. the bare atom ground state. Similarly, the excited dressed states are shifted by $\Delta_{1e} = (\Omega_c - |\delta_c|)/2$ and $\Delta_{2e} = -(\Omega_c + |\delta_c|)/2$ w.r.t. the bare atom excited state. Here, δ_c is the cooling beam detuning, $\Omega_c = \sqrt{(\delta_c)^2 + (\Omega_{c0})^2}$, and Ω_{c0} is the on-resonant Rabi frequency due to the cooling beams. In the limit of high detunings, the ground state shifts can be approximated as $\Delta_{1g} = -\Omega_{c0}^2/(4|\delta_c|)$ and $\Delta_{2g} = |\delta_c| + \Omega_{c0}^2/(4|\delta_c|)$. Dressed atom spectroscopy has been investigated in detail by several groups earlier, see [27, 28].

Thus, as the frequency of the excitation laser is scanned (during the one- or two-photon excitation) within a MOT, there are two possible resonances, namely $\Delta_{1g} \rightarrow$ excited state (Δ_1 resonance) and $\Delta_{2g} \rightarrow$ excited state (Δ_2 resonance). In the one-photon excitation, see figure 7(a), we observe that the larger (D1) and smaller dips (D2) in the 795 nm fluorescence signal are approximately at the frequencies of the Δ_1 and Δ_2 resonances. From this, we speculate that the dip, which is shifted by a few MHz from the $5S_{1/2} F = 2 \rightarrow 5P_{1/2} F' = 2$ resonance, is due to the pushing of the atoms occurring at the Δ_1 resonance. The pushing effect at the Δ_2 resonance appears much smaller than that at Δ_1 . Simple calculations based on the dressed atom may not give accurate predictions because our system is rather complicated. However, such calculations provide the correct orders of magnitude and trends. For example, by taking the MOT cooling beam intensities as 66 mW cm^{-2} , cooling detuning as -14 MHz (and saturation intensity 3 mW cm^{-2}), we calculated the ground state shifts, Δ_{1g} and Δ_{2g} , to be -4.5 MHz and $+18.5 \text{ MHz}$, respectively. This corresponds to the positions of the Δ_1 and Δ_2 resonances at $+4.5 \text{ MHz}$ and -18.5 MHz , respectively. In the experiments, we observed dips at D1 from $+1$ to $+12 \text{ MHz}$ and at D2 from -10 to -24 MHz . These values agree within an order of magnitude with the calculated ones. Additionally, by changing the cooling beam intensities, we observed that the frequency shift trends of the D1 resonances followed those that we would expect based on our speculations.

The pushing effect is much more significant when atoms are near the ONF, probably since the field intensity is much higher and there is much more light scattering in this region. Both

for the one- and two-photon excitation processes, the broad fluorescence profile with a relatively narrower dip is due to a varying power broadening and a varying pushing effect in the evanescent field due to its exponential profile. We emphasise that the two-peak profile is observed only for the excitation of atoms near a fibre surface. When the detection is also via the nanofibre, the dip is more pronounced and broader. This may be due to higher scattering and pushing near the fibre surface and probing it efficiently via the nanofibre itself. In contrast, when atoms are far away from the ONF, detection is done using a PMT which gives the collective signal from the MOT. We observe a small dip at $\sim -14 \text{ MHz}$ but the positive side dip (D1) is not visible, see the PMT signals in figures 9(a) and (b).

During these studies, we came to know that a similar spectrum has been observed with Cs atoms in a MOT near an ONF [18, 29] where the authors did the following experiments. For a single-atom condition near the ONF, a probe laser in a travelling wave arrangement was focussed perpendicular to the fibre axis. Fluorescence collected from the ONF showed a sharp dip (narrower than the natural linewidth) as the probe frequency was scanned across the resonance. The authors speculated that the effect arose from the shifting of the MOT centre due to pushing by the probe beam, thereby changing the local density of the atom cloud. Another hypothesis for the observed spectrum was quantum interference and the result was attributed to atom trapping with motional quantisation [30]. Our results support the former hypothesis though our results are neither limited to the single-atom condition nor one-photon excitation. Additionally, our studies show that this effect is present when light propagates through the nanofibre either in a travelling wave or counter-propagating arrangement.

5. Conclusion

We have experimentally investigated the origin of the two-peak profile of a fluorescence signal when intense, single-frequency two-photon excitation light interacts with cold atoms near an ONF. To understand the origin of this profile, we performed experiments using one-photon excitation for atoms both near and far from the nanofibre. Observations indicate that a similar profile is present when one-photon excitation is performed near the ONF. We speculate that, at higher excitation powers, resonance scattering induced pushing near the nanofibre becomes the dominant effect. This sharply depletes the atom number density, giving rise to a dip in the fluorescence. The frequency position of the resonance is modified due to the laser cooling beams; hence, the dip is slightly shifted from the bare atom resonance. This hypothesis also explains the similarity of profiles obtained in the presence and absence of cooling beams during two-photon excitation. This is due to pushing, or loss, of the atoms in a MOT, resulting in a lower initial atom number in the molasses phase. The dip is also observed in the molasses phase. These observations are crucial for near-resonant, high-intensity experiments based on the cold atom-nanofibre platform in order to better understand the spectral profiles obtained.


Acknowledgments

This work was supported by the Okinawa Institute of Science and Technology Graduate University and JSPS KAKENHI (Grant-in-Aid for Scientific Research (C)) 19K05316. SNC acknowledges support by Investments for the Future from LabEx PALM (ANR-10-LABX-0039-PALM). The authors thank A M Akulshin, J L Everett, H-H Jen, J Mompert, K P Nayak and J Robert for insightful discussions, and T Ray and K Subramonian Rajasree for their early studies that inspired this work.

Data availability statement

The data generated and/or analysed during the current study are not publicly available for legal/ethical reasons but are available from the corresponding author on reasonable request.

ORCID iDs

Vandna Gokhroo  <https://orcid.org/0000-0001-7614-2521>
 Fam Le Kien  <https://orcid.org/0000-0002-3463-6053>
 Síle Nic Chormaic  <https://orcid.org/0000-0003-4276-2014>

References

- [1] Cohen-Tannoudji C, Dupont-Roc J and Grynberg G 1998 *Atom-Photon Interactions: Basic Processes and Applications* (New York: Wiley)
- [2] Agarwal G S 2012 *Quantum Optics* (Cambridge: Cambridge University Press)
- [3] Fleischhauer M, Imamoglu A and Marangos J P 2005 *Rev. Mod. Phys.* **77** 633–73
- [4] Fulton D J, Shepherd S, Moseley R R, Sinclair B D and Dunn M H 1995 *Phys. Rev. A* **52** 2302–11
- [5] Kumar R, Gokhroo V and Nic Chormaic S 2015 *New J. Phys.* **17** 123012
- [6] Goban A, Choi K S, Alton D J, Ding D, Lacroûte C, Pototschnig M, Thiele T, Stern N P and Kimble H J 2012 *Phys. Rev. Lett.* **109** 033603
- [7] Lee J, Grover J A, Hoffman J E, Orozco L A and Rolston S L 2015 *J. Phys. B: At. Mol. Opt. Phys.* **48** 165004
- [8] Nieddu T, Gokhroo V and Nic Chormaic S 2016 *J. Opt.* **18** 053001
- [9] Kien F L, Nic Chormaic S and Busch T 2021 *Phys. Rev. A* **103** 063106
- [10] Gupta R K, Everett J L, Tranter A D, Henke R, Gokhroo V, Lam P K and Nic Chormaic S 2021 Machine learner optimization of optical nanofiber-based dipole traps for cold ^{87}Rb atoms (arXiv:2110.03931)
- [11] Ray T, Gupta R K, Gokhroo V, Everett J L, Nieddu T, Rajasree K S and Nic Chormaic S 2020 *New J. Phys.* **22** 062001
- [12] Hinney J, Prasad A S, Mahmoodian S, Hammerer K, Rauschenbeutel A, Schneeweiss P, Volz J and Schemmer M 2021 *Phys. Rev. Lett.* **127** 123602
- [13] Rajasree K S, Gupta R K, Gokhroo V, Kien F L, Nieddu T, Ray T, Nic Chormaic S and Tkachenko G 2020 *Phys. Rev. Res.* **2** 033341
- [14] Kumar R, Gokhroo V, Deasy K and Nic Chormaic S 2015 *Phys. Rev. A* **91** 053842
- [15] Kien F L, Dutta Gupta S, Balykin V I and Hakuta K 2005 *Phys. Rev. A* **72** 032509
- [16] Sagué G, Vetsch E, Alt W, Meschede D and Rauschenbeutel A 2007 *Phys. Rev. Lett.* **99** 163602
- [17] Nayak K P, Melentiev P N, Morinaga M, Kien F L, Balykin V I and Hakuta K 2007 *Opt. Express* **15** 5431–8
- [18] Nayak K P and Hakuta K 2008 *New J. Phys.* **10** 053003
- [19] Ward J M, Maimaiti A, Le V H and Nic Chormaic S 2014 *Rev. Sci. Instrum.* **85** 111501
- [20] Safronova M S and Safronova U I 2011 *Phys. Rev. A* **83** 052508
- [21] Nieddu T, Ray T, Rajasree K S, Roy R and Nic Chormaic S 2019 *Opt. Express* **27** 6528–35
- [22] Russell L, Gleeson D A, Minogin V G and Nic Chormaic S 2009 *J. Phys. B: At. Mol. Opt. Phys.* **42** 185006
- [23] Zibrov A S, Lukin M D, Nikonov D E, Hollberg L, Scully M O, Velichansky V L and Robinson H G 1995 *Phys. Rev. Lett.* **75** 1499–502
- [24] Hopkins S A, Usadi E, Chen H X and Durrant A V 1997 *Opt. Commun.* **138** 185–92
- [25] Cardimona D A, Raymer M G and Stroud C R 1982 *J. Phys. B: At. Mol. Phys.* **15** 55–64
- [26] Agarwal G S 2000 *Phys. Rev. Lett.* **84** 5500–3
- [27] Mitsunaga M, Mukai T, Watanabe K and Mukai T 1996 *J. Opt. Soc. Am. B* **13** 2696–700
- [28] Wu F Y, Ezekiel S, Ducloy M and Mollow B R 1977 *Phys. Rev. Lett.* **38** 1077–80
- [29] Nayak K P 2009 Single photon generation and spectroscopy using quantum dots on optical nanofibers *PhD Thesis* The University of Electro-Communications, Tokyo.
- [30] Hakuta K 2008 Single atoms on an optical nanofiber: a novel work system for slow light *Advances in Slow and Fast Light Proc. SPIE 6904* ed S M Shahriar, P R Hemmer and J R Lowell (San Jose, California, United States) pp 19–23